ISSN 1810-2328, Journal of Engineering Thermophysics, 2015, Vol. 24, No. 3, pp. 237–246. © Pleiades Publishing, Ltd., 2015.

# Effect of the Content of Salt Admixtures on Integral Characteristics of Evaporation of Water Drops Moving through High-Temperature Gas Media

**R. S. Volkov[*], G. V. Kuznetsov[**], and P. A. Strizhak[***]**

*National Research Tomsk Polytechnic University, pr. Lenina 30, Tomsk, 634050 Russia*

Received October 11, 2013

**Abstract**—Experimental research on the influence of the content of typical salt admixtures in water on integral characteristics of its evaporation while moving through a high-temperature gas medium was carried out using NaCl nanopowder. Experiments were conducted with single large (more than 1 mm) drops and an aggregate of (more than one hundred) small (under 0.3 mm) water droplets moving through a channel filled with high-temperature combustion products. Conditions were determined under which the content of salt admixtures in water has a strong effect (the decrease of mass changes several times) on the intensity of evaporation of the latter in the region of high-temperature gases.

**DOI:** 10.1134/S1810232815030054

## INTRODUCTION

In recent years, much attention is given to technologies of usage of escaping flue gases (combustion products of various fuels and substances in power plants) [1–6]. For example, we can note new technologies of gas-vapor heat carriers (mixtures of flue gases and water vapors) [1, 2], energy-efficient cleaning, degreasing, treatment and painting of surfaces of various products [3, 4], and also defrosting of dry substances by high-temperature vapor-gas mixtures [5, 6]. For vapor generation, these technologies often use liquids of different composition [1–6]. The most widely used working liquid is water [1–6]. In different reservoirs, storages, and makeup systems, its composition is often substantially different, particularly, by the content of salts that can significantly affect the vaporization process [7]. Until now, the mechanisms of probable effect of salts on the change in composition of gas-vapor flows in technologies have not been sufficiently studies [1–6]. This is of particular importance for highly sensitive systems of product surface processing [3, 4] and also for better understanding of the processes of motion of complex gas, liquid, vapor-gas, and vapor-liquid mixtures, their flowing onto obstacles of different geometries and collision with surfaces [8–17].

For studying the effect of salt admixtures on the evaporation intensity of single drops and dispersed water in the region of high-temperature gases and the content of the formed gas-vapor flow, one can use experimental methods [18, 19] with application of optical methods for diagnostics of two-phase flows (in particular, particle image velocimetry (PIV) and interferometric particle imaging (IPI) [20–22]). Results of experiments [18, 19] carried out using PIV and IPI methods have made it possible to obtain good agreement with theoretical inferences of numerical investigations [23, 24]. In particular, authors of [18, 19] have found a slight decrease (about 3–5%) in sizes of quite large (larger than 1 mm) water drops moving through the region (1 m long) of high-temperature (to 1100 K) combustion products. For fine-dispersed (initial drop sizes under 0.1 mm) water flows in identical environments, conditions of practically complete evaporation were identified [18, 19]. It is of interest to experimentally investigate

[*]E-mail: romanvolkov@tpu.ru
[**]E-mail: elf@tpu.ru
[***]E-mail: pavelspa@tpu.ru

the influence of salt content in water on its evaporation intensity while moving in the region of high-temperature gases as a flow of dispersed liquid and large (more than 1mm) solid drops with application of the equipment and methods [18, 19].

This work is aimed at experimental estimation of the effect of salt content in water on the integral characteristics of its evaporation while moving through high-temperature combustion products.

## EXPERIMENTAL SETUP AND METHODS OF RESEARCH

We used the setup (Fig. 1) [18, 19] consisting of a cross-correlation video camera, 2048 × 2048 pixels, no less than 1.5 Hz of vertical refresh rate, delay between two successive frames, under 5 $\mu$s; double pulsed solid-state Nd-YAG laser at 532 nm, pulse energy no less than 70 mJ, pulse length under 12 ns, pulsed laser frequency under 15 Hz; sync processor, sampling rate under 10 ns.

The working liquid was water with special inclusions, that is, "tracers," representing admixture (relative mass concentration (fraction) is 0.5%) of titanium dioxide nanopowder to enhance contrast of videograms obtained by the cross-correlation camera. The $TiO_2$ nanoparticles were chosen as the tracers because they do not dissolve in water [25]. The working liquid contained also NaCl nanoparticles (the relative mass concentration varied in the range $\gamma = 0–10\%$) to study the influence of typical salt admixtures on the water evaporation characteristics.

For each value of $\gamma$, the cycle of experiments included two series, ten experiments each. In the first series of experiments we fixed video frames of dispersed liquid at the inlet to cylinder channel *13* (1 m high, 0.3 m in diameter). In the second series, we recorded images of drops after they had passed the flame zone. Each series of the experiments consisted of several stages:

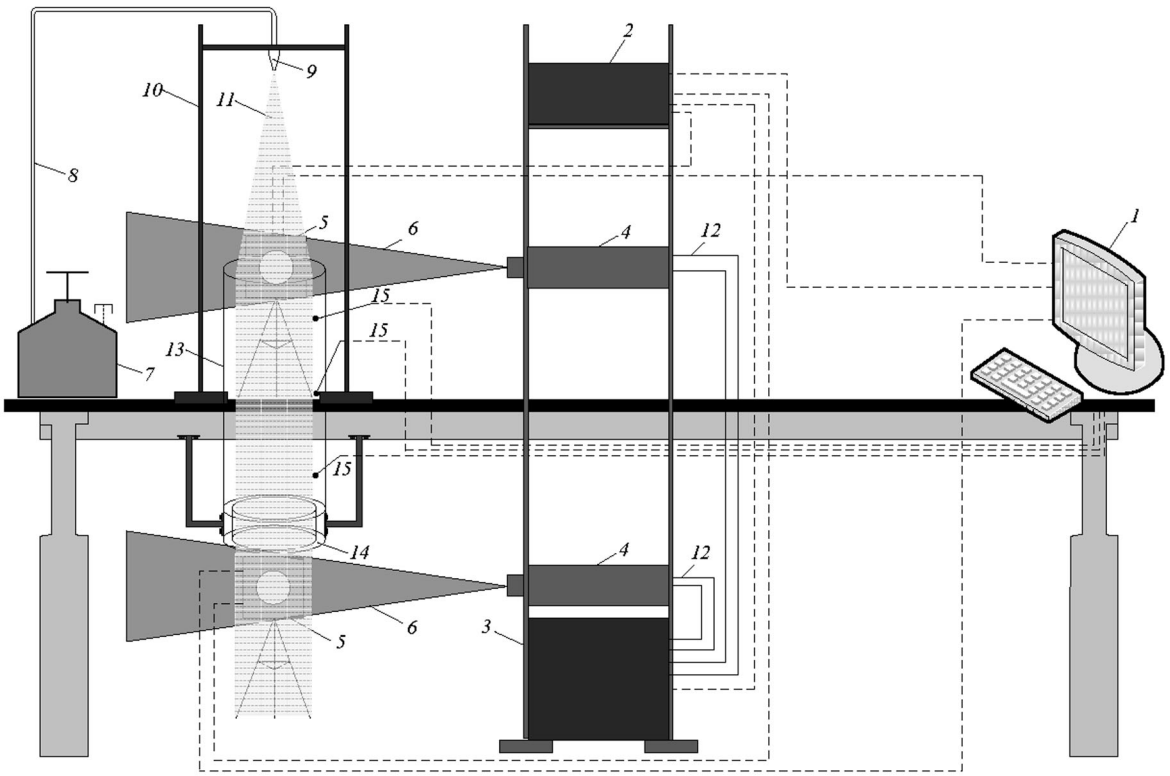


**Fig. 1.** A scheme of the experimental setup: *1*—PC; *2*—synchronizer of PC, cross-correlation camera, and laser; *3*—laser radiation generator; *4*—double solid pulsed laser; *5*—cross-correlation camera; *6*—fin; *7*—vessel with working liquid; *8*—working liquid; *9*—disperser; *10*—support; *11*—working liquid drops; *12*—channel of movement of cooling laser liquid; *13*—cylinder of heat-resistant translucent material; *14*—hollow cylinder with fuel liquid filled in the interwall space; *15*—thermocouples.

—liquid was poured into vessel *7* (the composition was varied: NaCl—0–10%, $H_2O$—89.5–99.5%, $TiO_2$—0.5%);

—disperser *9*, adjusted to required liquid dispersion parameters, was connected to the outlet of vessel *7*;

—vessel *7* with disperser *9* was mounted on support *10*, 0.5 m higher than the upper edge of cylinder *13* (this location was chosen to protect disperser *9* against fusion under the action of high-temperature combustion products emerging from cylinder channel *13*);

—the height of the support of cross-correlation camera *5* and also the height of mounting of laser *4* were chosen such that the optic axis of the camera and the plane of laser fin *6* intersect at an angle of 90 deg and the point of their intersection is in the working zone;

—the cross-correlation camera *5* was calibrated (the scale factor to be determined on PC *1*), the "waist" of fin *6* of laser *4* was adjusted;

—the base of hollow cylinder *14* was filled with typical liquid combustible substance (about 250 ml), which was fired prior to the experiment;

—after 5 min burning (the time needed for heating the inner cavity of cylinder *13* to $1070 \pm 30$ K), special software was launched on PC *1*, disperser *9* was switched on, and recording of videograms was performed in the chosen working region;

—the obtained video frames were used to determine drop sizes, calculate velocity fields of the dispersed liquid tracers, and values of drop velocities (before and after the high-temperature zone).

To form stable flame in the experiments, we used typical liquid fuel with stable properties, namely, kerosene. While combustion of kerosene, a high-temperature flow of combustion products (flue gases) was generated in cylinder channel *13*, and water drops passed trough it.

While processing the video frames, we used methods of digital tracer visualization, PIV and IPI [20–22]. Measurement of the instantaneous velocity field at the given section is based on recording the displacement of admixture particles, that is, tracers, being in the section plane, in the fixed time period. The measurement region of the dispersed flow was the plane of the laser fin (Fig. 1). The tracers were repeatedly illuminated. The tracer patterns were recorded by the digital video camera. Subsequent processing of the images made it possible to calculate displacements of the particles during the time period between two flashes of the light source and the tracer velocity [20–22].

While processing the experimental videograms by methods [20–22] we calculated the scale factor $S$, which was 0.004 mm/pixel for the investigated working regions (at the inlet and outlet of the channel with the high-temperature gas flow). The videograms were divided into recoding regions of $32 \times 32$ pixels, after that for each of the latter we calculated the correlation function. The correlation function maximum corresponded to the most probable shift of the particles in this zone according to [20–22]. It was supposed that the flow velocity in the elementary region is constant and that displacements of all particles are identical, i.e., the correlation function has one most prominent maximum against possible noises [22]. Simultaneously with finding the maximum correlation function for decreasing the number of random correlations related to the effect of "lost pair" we applied the superimposed top-hat window [20, 21] and, thus, reduced the contribution to the correlation function from particles located in the immediate vicinity from the boundaries of the video frame calculation domain. With the known time delays between laser flashes and the most probable displacements of particles (calculated by the maximum correlation function) in the recording regions of the video frames we found the instantaneous tracer velocities [20–22].

While processing the videograms of the experiments, we also applied procedures with the use of weight functions [20, 21]: No–DC (to eliminate the constant component in the signal) and Low–pass (to increase the width of correlation peaks due to cutoff of a small part of low frequencies and a considerable part of high frequencies from the correlation function spectrum). In addition, we threw away some part of the obtained vectors by the signal-to-noise ratio (peak validation function) [20, 21].

In the flow of dispersed liquid the sizes of drops varied in the range $0.04 \le R \le 0.37$ mm. In the processing of videograms for estimating the change in the integral evaporation characteristics of drops the latter were conventionally subdivided in sizes into several groups: 1—$0.04 \le R \le 0.09$ mm, 2—$0.09 < R \le 0.16$ mm, 3—at $0.16 < R \le 0.23$ mm, 4—at $0.23 < R \le 0.3$ mm, 5—at $0.3 < R \le 0.37$ mm.

The drop sizes in the calculation domains of videograms (before and after the high-temperature gas channel) were determined by the IPI method [22]. The flow of drops was illuminated repeatedly by fin *6* of laser *4*; at that, we observed interference between the light reflected and refracted by the drops. The procedure of image video recording was performed by cross-correlation camera *5*. Then we determined the drop size in the flow by the number of interference fringes observed on the videograms [22].

Chromel-copel thermocouples controlled the temperature of combustion products (flue gases) $T_f$ in cylinder channel *13* ($1150 \pm 30$ K). We used the technique of thermocouple measurements [26]. The systematic errors of measuring $T_f$ were under 2.5% [27], for drop sizes they were 0.001 mm [28], and 2% for tracer velocities [20, 21].

## RESULTS AND DISCUSSION

In the experimental research, we recorded video images of dispersed liquid drops at the inlet and outlet from the zone of high-temperature combustion products and analyzed changes in the dispersion of two-phase vapor-liquid mixture. The results of videogram processing were used to calculate velocity fields of tracers and calculate from them velocities of single liquid drops. Typical videograms and the related velocity fields of tracers for the series of experiments with $\gamma = 10\%$ are shown in Fig. 2.

Using the results of videogram processing, we determined the integral characteristics of the dispersed vapor-liquid flow moving through the zone of high-temperature gases (the change in the characteristic size of drops $R_m$, their velocity $u_m$, and relative concentration in the regions of registration of videoframes $\alpha_m$). Table 1 presents results of processing a series of videograms with $\gamma = 10\%$.

It has been found that during movement of the dispersed liquid through the flame, there occurs a significant change in the composition of the gas- and vapor-liquid mixture (Table 1). Liquid drops of group no. 1 ($r \le 0.09$ mm) are absolutely absent at the outlet from the high-temperature gas region ($\alpha_m \to 0$). Drops of group no. 2 ($0.09 < R \le 0.16$ mm) are evaporated, on average, by 47%, those of group no. 3 ($0.16 < R \le 0.23$ mm)—by 30%, of group no. 4 ($0.23 < R \le 0.3$ mm)—by 23%, of group no. 5 ($0.3 < R \le 0.37$ mm)—less than by 17%. As a result, in the working region at the outlet from the zone of high-temperature gases, the liquid drop concentration $\alpha_m$ is much lower than at the inlet (Table 1). This is evident from Fig. 2.

The experiments have also shown that the movement velocities of the considered groups of drops are substantially different. Drops with characteristic sizes $R \le 0.16$ mm (groups no. 1 and no. 2) move much slower ($u_m \to 0$) relative to the initial velocity and are evaporated almost completely. For drops of group no. 3, the $u_m$ decreases by 35–40% relative to the initial values, for drops of group no. 4—by

**Table 1.** Integral characteristics of movement of dispersed liquid drops with salt fraction $\gamma = 10\%$

| Parameter | Group no. | At channel inlet | At channel outlet |
|---|---|---|---|
| $R_m$, mm | 1 | 0.085 | 0 |
| | 2 | 0.136 | 0.085 |
| | 3 | 0.195 | 0.143 |
| | 4 | 0.247 | 0.196 |
| | 5 | 0.324 | 0.252 |
| $\alpha_m$, % | 1 | 1.33 | 0 |
| | 2 | 22.00 | 2.80 |
| | 3 | 46.00 | 9.06 |
| | 4 | 24.66 | 47.73 |
| | 5 | 6.02 | 40.41 |
| $u_m$, m/s | | 0.852 | 0.342 |

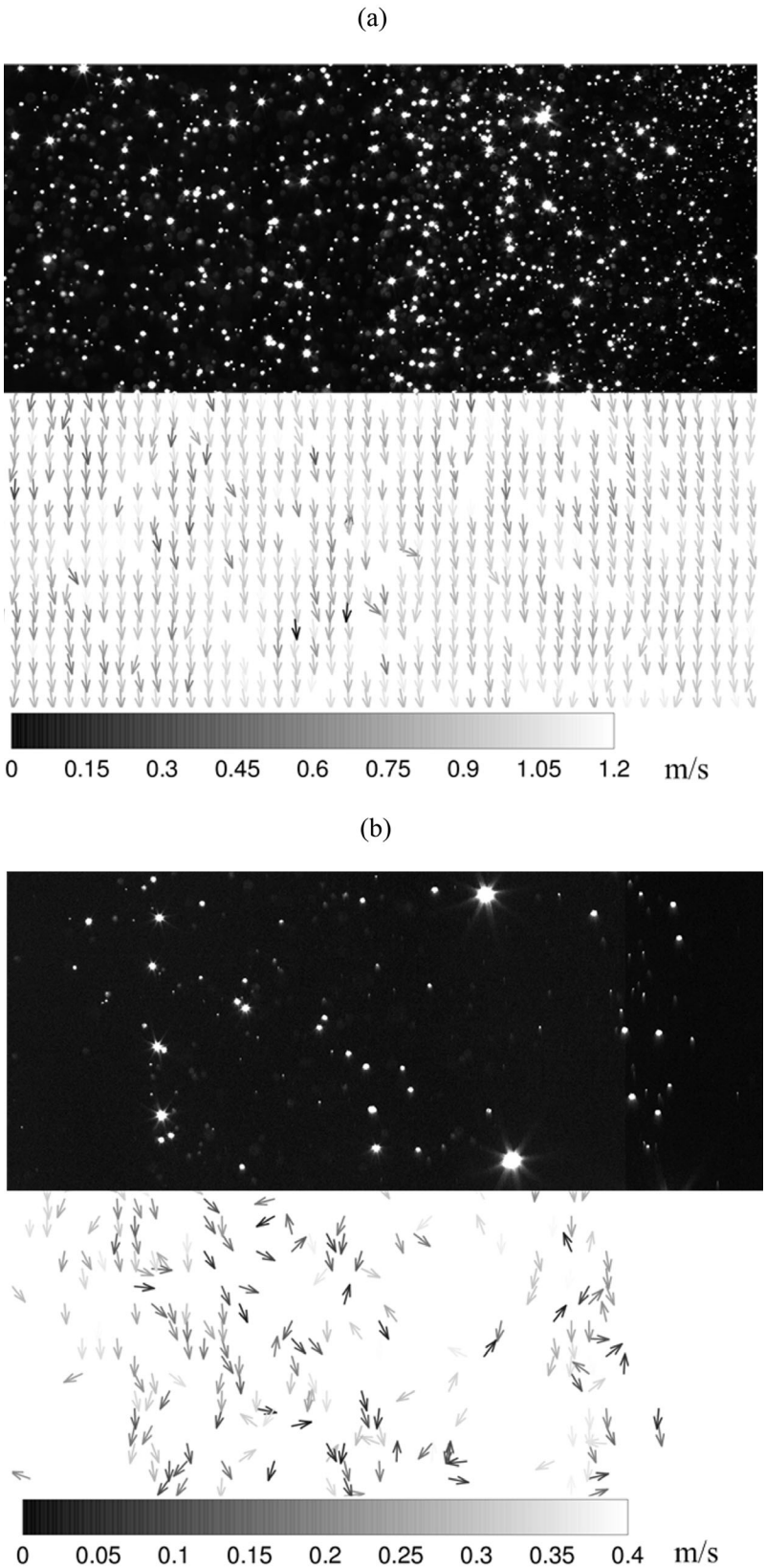


**Fig. 2.** Videograms of dispersed liquid drops and velocity fields of tracers at the inlet (a) and outlet (b) from the high-temperature gas zone with $\gamma = 10\%$.

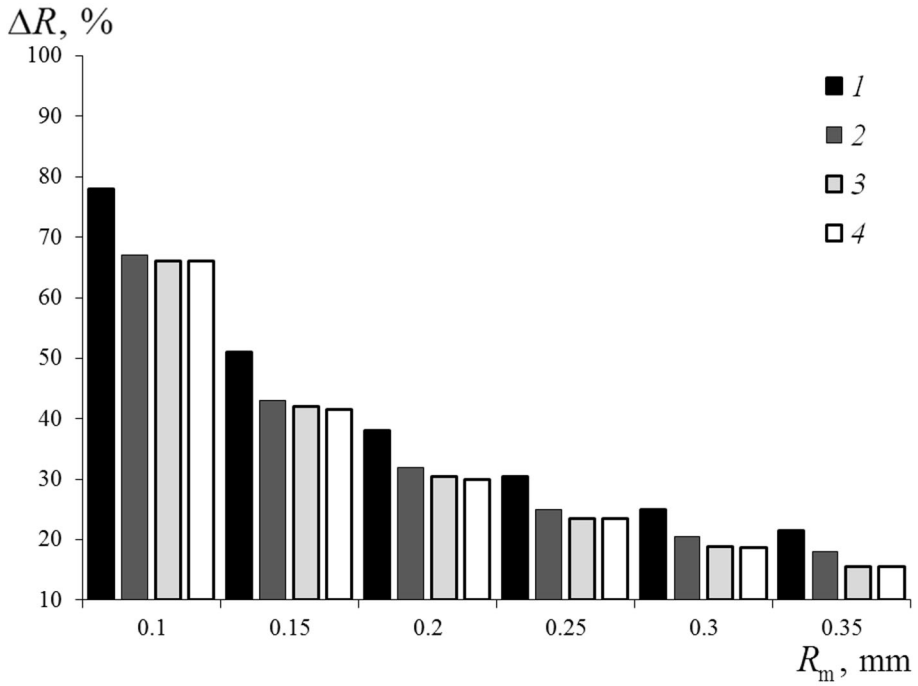


**Fig. 3.** Parameter $\Delta R$ versus initial size of drops $R_{\rm m}$: *1*—with $\gamma = 0\%$, *2*—with $\gamma = 2.5\%$, *3*—$\gamma = 5\%$, *4*—$\gamma = 10\%$.

15–17%, and for drops of group no. 5—by 13–15%. The obtained results are in good agreement with the main inferences of the experiments [18, 19].

The characteristics of motion of dispersed liquid drops ($R_{\rm m}$, $\alpha_{\rm m}$, and $u_{\rm m}$), presented in Table 1, were calculated for several values of $\gamma$ varying from 0 to 10%. In processing of the calculated values of $R_{\rm m}$, we obtained the dependences of the parameter $\Delta R$ characterizing the relative change in the size of drops moving through the high-temperature gas medium on their initial radius for $\gamma = 0$–10% (Fig. 3).

It is seen (Fig. 3) that for the dispersed liquid drops with characteristic sizes $R_{\rm m} < 0.4$ mm the effect of salt content with $\gamma = 0$–10% is insignificant (the change in $\Delta R$ is under 5%). This can be explained by the fact that as the size of a "salt" water drop decreases, the number of NaCl particles in the drop volume is reduced. As a result, the specific heat of the drop, as the "$H_2O$ + NaCl" system, decreases. Less energy is required for heating of the surface layer of the system and intensification of phase transition. Consequently, the integral characteristics of vaporization are almost adequate (Fig. 3) to dispersed water without salt admixtures ($\gamma = 0\%$).

Figure 4 represents the parameter $\Delta R$ versus $R_{\rm m}$ and $\gamma$ as a surface separating the regions of intensive (the decrease in the mean sizes of drops during water evaporation is more than by 30–40%) and moderate (the change in the sizes of drops is under 10–15%) vaporization in the zone of high-temperature gases. For instance, if $R_{\rm m}$ and $\gamma$ correspond to parameters of $\Delta R$ above the surface, intensive evaporation conditions are realized. For parameters $R_{\rm m}$ and $\gamma$, characterizing the $\Delta R$ values under the surface, moderate vaporization and, consequently, an insignificant change in the dispersion of the vapor-gas mixture in the high-temperature gas zone are typical.

We also carried out experiments on studying the effect of salt concentration $\gamma$ on the integral characteristics of evaporation of large liquid drops with an initial mean radius of 2–4 mm. In the experimental setup (Fig. 1), we used a feeder instead of the disperser [18, 19].

Figure 5 presents typical videograms with single drops at boundaries of the high-temperature gas zone with $\gamma = 10\%$ and $R_{\rm d} = 2.905$ mm. It is clearly seen that the change in the size of drops is more moderate ($\Delta R < 10\%$) compared to the dispersed flow (Fig. 2).

Table 2 presents results of processing of series consisting of ten experiments with $\gamma = 10\%$ and $\gamma = 0\%$ for drops with a medium radius of about 3 mm. It is shown that in spite of the less intensive evaporation (the result is in good agreement with the experimental data [18, 19]), for large drops the

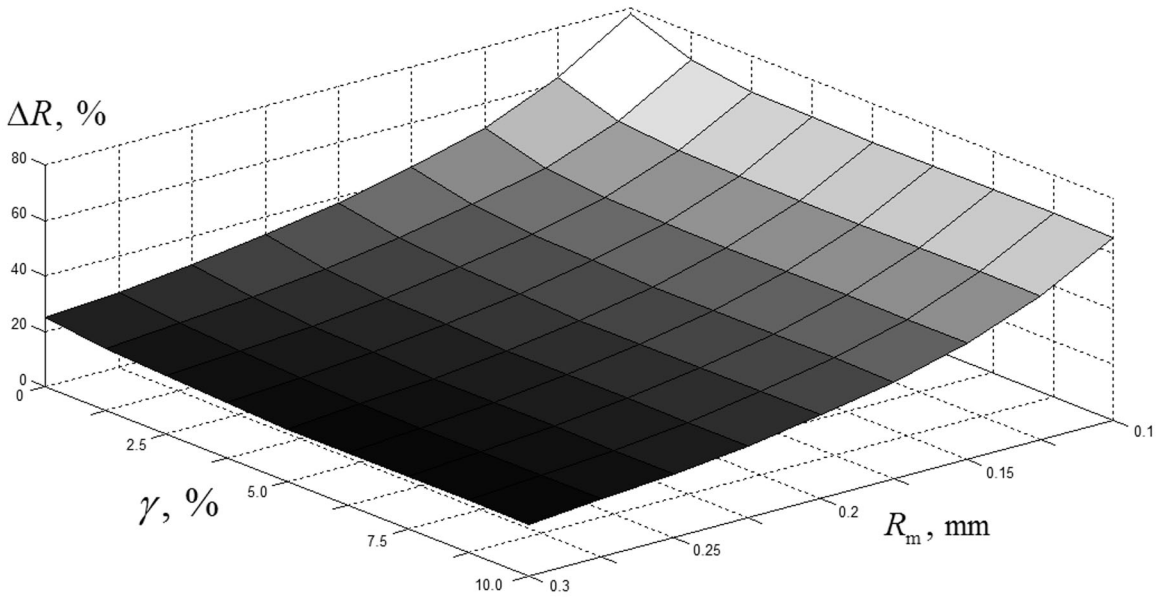


**Fig. 4.** Parameter $\Delta R$ versus salt fraction $\gamma$ and initial sizes $R_{\mathrm{m}}$ of liquid drops.

**Table 2.** Averaged sizes of single liquid drops with salt fraction $\gamma = 10\%$ and $\gamma = 0\%$ before ($R_{\mathrm{d}}$) and after ($R^*_{\mathrm{d}}$) passage through high-temperature combustion products

| Experiment no. | $\gamma = 10\%$ | | | $\gamma = 0\%$ | | |
|---|---|---|---|---|---|---|
| | $R_{\mathrm{d}}$, mm | $R^*_{\mathrm{d}}$, mm | $\Delta R_1$, % | $R_{\mathrm{d}}$, mm | $R^*_d$, mm | $\Delta R_2$, % |
| 1 | 2.906 | 2.882 | 0.826 | 2.902 | 2.712 | 6.564 |
| 2 | 2.907 | 2.895 | 0.413 | 2.905 | 2.741 | 5.663 |
| 3 | 2.906 | 2.88 | 0.895 | 2.906 | 2.729 | 6.091 |
| 4 | 2.905 | 2.89 | 0.516 | 2.904 | 2.729 | 6.010 |
| 5 | 2.906 | 2.889 | 0.585 | 2.905 | 2.730 | 6.024 |
| 6 | 2.905 | 2.891 | 0.482 | 2.906 | 2.718 | 6.487 |
| 7 | 2.905 | 2.874 | 1.067 | 2.904 | 2.745 | 5.492 |
| 8 | 2.906 | 2.888 | 0.619 | 2.907 | 2.714 | 6.656 |
| 9 | 2.904 | 2.886 | 0.620 | 2.905 | 2.732 | 5.955 |
| 10 | 2.904 | 2.875 | 0.999 | 2.907 | 2.715 | 6.605 |

influence of $\gamma$ is more significant (the relative differences for $\Delta R_1$ and $\Delta R_2$ reach 80–92%) than for dispersed vapor-liquid flows. This is caused by the fact that while moving a certain "solid" mass of water with salt admixtures the effect of NaCl particles becomes significant (first of all, heat capacity of the "$H_2O$ + NaCl" system grows). As a result, energy spent on heating of the surface layer of the "$H_2O$ + NaCl" system and on the phase transition is increased—evaporation is less intensive.

At the same time, we should note that in the experiments for dispersed liquid drops with the initial size under 0.1 mm, only tracers with NaCl particles were recorded at the outlet from the flame zone (Fig. 2). This peculiarity shows that by decreasing substantially the size of drops of water with NaCl admixtures, despite high values of $\gamma$, one can significantly intensify vaporization and practically "eliminate" the liquid phase. This feature of the process shows that the degree of diminishing the water drops, e.g.,

(a)

(b)

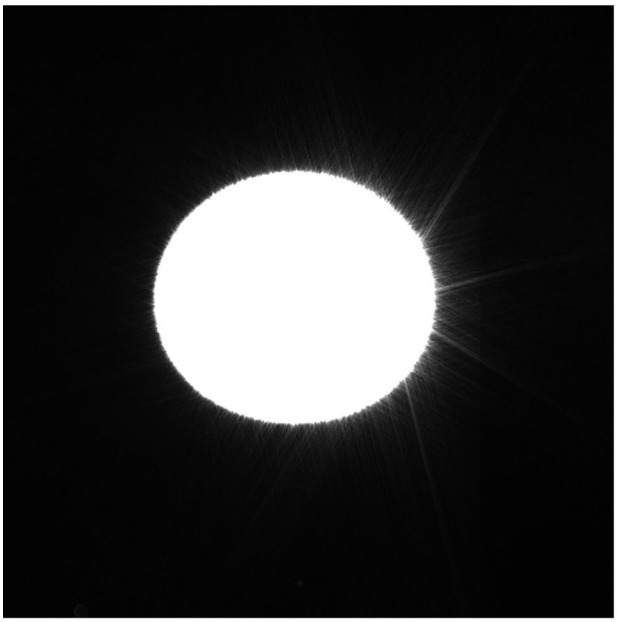

**Fig. 5.** Videograms of single liquid drops with the initial size $R_d = 2.905$ mm at the inlet (a) and outlet (b) from the high-temperature gas zone with $\gamma = 10\%$.

for technologies [1–6], has to be chosen according to the required composition (relative concentrations of the main components and admixtures) of gas-vapor and vapor-liquid mixtures.

## CONCLUSIONS

As a result of the experimental research, we have found that in the case of fine dispersed (achieving a drop size of several hundreds of micrometers) water with a varying salt content ($\gamma = 0$–$10\%$), it

is possible to attain conditions under which the integral vaporization characteristics will be almost adequate (deviations under 5%) to water without corresponding admixtures. This result allows us to conclude that it is possible to use water from water pools and storage basins with different salt content in some technologies using gas-vapor and vapor-liquid admixtures, e.g., [1–6].

## ACKNOWLEDGMENTS

This research was supported by the Russian Foundation for Basic Research (grant no. 14-08-00057).

## NOTATIONS

$R$—drop radius, mm

$R_{\mathrm{d}}$—radius of large single liquid drops at the inlet to the flame zone, mm

$R_{\mathrm{d}}^{*}$—radius of large single liquid drops at the outlet from the flame zone, mm

$R_{\mathrm{m}}$—mean characteristic radius of dispersed small drops, mm

$R_{\mathrm{m}}^{*}$—radius of group of liquid drops at the outlet from the flame zone, mm

$\Delta R$—parameter characterizing relative change in sizes of drops while moving through a high-temperature gas medium versus their initial radius, %

$S$—scale factor, mm/pixel

$T_{\mathrm{f}}$—temperature of combustion products, K

$u_{\mathrm{m}}$—mean velocity of drops, m/s

$\alpha_{\mathrm{m}}$—mean relative concentration, %

$\gamma$—relative mass concentration, %

## REFERENCES

1. Nikitin, M.N., The Effect of Water Injection in Heat Generator on the Pressure of Vapor-Gas Mixture, *Prom. Energ.*, 2010, no. 6, pp. 42–46.
2. Nikitin, M.N., Usage of Vapor-Gas Admixture in Fuel Combustion, *Prom. Energ.*, 2010, no. 12, pp. 37–42.
3. Ibatullin, I.D., *Kinetika ustalostnoi povrezhdaemosti i razrusheniya poverkhnostnykh sloev* (Kinetics of Fatigue Damage and Breaking of Surface Layers), Samara: SGTU, 2008.
4. Maryin, B.N., Kim, V.A., and Sysoev, O.E., *Obrabotka poverkhnostei v metallurgii i mashinostroenii* (Surface Treatment in Metallurgy and Machine Building), Vladivostok: Dal'nauka, 2011.
5. Pershin, V.F., Odnolko, V.G., and Pershina, S.V., *Pererabotka sypuchikh materialov v mashinakh barabannogo tipa* (Processing of Bulk Solids in Drum-Type Machines), Moscow: Mashinostroenie, 2009.
6. Isaev, E.A., Chernetskaya, I.E., Krakht, L.N., and Titov, V.S., *Teoriya upravleniya okomkovaniem sypuchikh materialov* (Theory of Control of Bulk Solid Balling), Staryi Oskol: TNT, 2012.
7. Isachenko, V.P., *Teploobmen pri kondensatsii* (Heat Transfer in Condensation), Moscow, Energiya, 1977.
8. Terekhov, V.I., Sharov, K.A., and Shishkin, N.E., Experimental Research of Mixing of a Gas Flow with Boundary Gas-Drop Jet, *Teplofiz. Aeromekh.*, 1999, vol. 6, no. 3, pp. 331–341.
9. Terekhov, V.I., Pakhomov, M.A., and Chichindaev, A.V., The Effect of Liquid Drop Evaporation on the Distribution of Parameters in Two-Component Laminar Flows, *Prikl. Mekh. Tekhn. Fiz.*, 2000, vol. 41, no. 6, pp. 68–71.
10. Terekhov, V.I., Yarygina, N.I., and Smulskii, Ya.I., Thermal and Dynamic Characteristics of Detached Flows behind a Flat Edge with Varying Orientation to the Flow, *Prikl. Mekh. Tekhn. Fiz.*, 2007, vol. 48, no. 1, pp. 103–109.
11. Maltsev, R.V. and Rebrov, A.K., Gas-Dynamic Colliders: Numerical Modeling, *Prikl. Mekh. Tekhn. Fiz.*, 2007, vol. 48, no. 3, pp. 142–151.
12. Ganesan, P. and Palani, G., Nonstationary Free-Convection Flowing around a Semi-Infinite Isothermal Vertical Plate with Mass Transfer, *Teplofiz. Aeromekh.*, 2005, vol. 12, no. 3, pp. 407–414.
13. Strizhak, P.A., Numerical Estimation of the Influence of Natural Convection in Liquid on the Conditions of Ignition by a Local Heat Source, *J. Eng. Therm.*, 2011, vol. 20, no. 2, pp. 211–216.
14. Ovcharova, A.S., The Influence of Thermophysical Properties of Liquid on the Peculiarities of Film Breaking under Thermal Load. The Role of Prandtl Number, *Appl. Mech. Tekhn. Fiz.*, 2012, vol. 53, no. 2, pp. 43–52.
15. Aktershev, S.P., Thermocapillary Waves in a Liquid Film, *J. Eng. Therm.*, 2012, vol. 21, no. 1, pp. 36–51.

16. Kuznetsov, V.V., Kozulina, I.A., and Vitovsky, O.V., Experimental Investigation of Adiabatic Evaporation Waves in Superheated Refrigerants, *J. Eng. Therm.*, 2012, vol. 21, no. 2, pp. 136–143.
17. Plotnikov, M.Yu. and Rebrov, A.K., Superzonic Flow of Rarefied Gas through a Wire Obstacle, *Prikl. Mekh. Tekhn. Fiz.*, 2013, vol. 54, no. 4, pp. 5–12.
18. Volkov, R.S., Vysokomornaya, O.V., Kuznetsov, G.V., and Strizhak, P.A., Experimental Investigation of the Laws of Fine-Dispersed Water Evaporation while Moving through High-Temperature Combustion Products, *Butler. Soobshch.*, 2013, vol. 35, no. 9, pp. 38–46.
19. Volkov, R.S., Vysokomornaya, O.V., Kuznetsov, G.V., and Strizhak, P.A., Experimental Study of the Change in the Mass of Water Droplets in Their Motion through High-Temperature Combustion Products, *J. Eng. Phys. Therm.*, 2013, vol. 86, no. 6, pp. 1413–1418.
20. Westerweel, J., Fundamentals of Digital Particle Image Velocimetry, *Meas. Sci. Technol.*, 1997, vol. 8, pp. 1379–1392.
21. Raffel, M., Willert, C., and Kompenhans, J., *Particle Image Velocimetry*, Berlin: Springer-Verlag, 1998.
22. Foucaut, J.M. and Stanislas, M., Some Considerations on the Accuracy and Frequency Response of Some Derivative Filters Applied to Particle Image Velocimetry Vector Fields, *Meas. Sci. Technol.*, 2002, vol. 13, pp. 1058–1071.
23. Strizhak, P.A., Influence of Droplet Distribution in a "Water Slug" on the Temperature and Concentration of Combustion Products in Its Wake, *J. Eng. Phys. Therm.*, 2013, vol. 86, no. 4, pp. 895–904.
24. Vysokomornaya, O.V., Kuznetsov, G.V., and Strizhak, P.A., Heat and Mass Transfer in the Process of Movement of Water Drops in a High-Temperature Gas Medium, *J. Eng. Phys. Therm.*, 2013, vol. 86, no. 1, pp. 62–68.
25. Ilyin, A.P., Nazarenko, O.B., Korshunov, A.V., and Root, L.O., *Osobennosti fiziko-khimicheskikh svoistv nanoporoshkov i nanomaterialov* (Peculiarities of Physical-Chemical Properties of Nanopowders and Nanomaterials), Tomsk: TPU, 2012.
26. Polezhaev, Yu.V. and Yuryevich, F.B., *Teplovaya zashchita* (Thermal Protection), Moscow: Mir, 1972.
27. Shenk, H., *Teoriya inzhenernogo eksperimenta* (Theory of Engineering Experiment), Moscow: Mir, 1972.
28. Zaidel, A.N., *Elementarnye otsenki oshibok izmereniya* (Elementary Estimate of Measurement Errors), 3d ed., USSR Acad. Sci., Leningrad: Nauka, 1968.